The *C. elegans* NF2/Merlin Molecule NFM-1 Non-Autonomously Regulates Neuroblast Migration and Interacts Genetically with the Guidance Cue SLT-1/Slit

Matthew P. Josephson, Rana Aliani, and Erik A. Lundquist[1]

The University of Kansas
Department of Molecular Biosciences
Program in Molecular, Cellular, and Developmental Biology
1200 Sunnyside Avenue
5049 Haworth Hall
Lawrence, KS 66046

[1]Corresponding Author (erikl@ku.edu)

Abstract

During nervous system development, neurons and their progenitors migrate to their final destinations. In *Caenorhabditis elegans,* the bilateral Q neuroblasts and their descendants migrate long distances in opposite directions, despite being born in the same posterior region. QR on the right migrates anteriorly and generates the AQR neuron positioned near the head, and QL on the left migrates posteriorly, giving rise to the PQR neuron positioned near the tail. In a screen for genes required for AQR and PQR migration, we identified an allele of *nfm-1*, which encodes a molecule similar to vertebrate NF2/Merlin, an important tumor suppressor in humans. Mutations in *NF2* lead to Neurofibromatosis Type II, characterized by benign tumors of glial tissues. These molecules contain Four-point-one Ezrin Radixin Moesin (FERM) domains characteristic of cytoskeletal-membrane linkers, and vertebrate NF2 is required for epidermal integrity. Vertebrate NF2 can also regulate several transcriptional pathways including the Hippo pathway. Here we demonstrate that in *C. elegans, nfm-1* is required for complete migration of AQR and PQR, and that it likely acts outside of the Q cells themselves in a non-autonomous fashion. We also show a genetic interaction between *nfm-1* and the *C. elegans Slit* homolog *slt-1*, which encodes a conserved secreted guidance cue. In vertebrates, *NF2* can control *Slit2* mRNA levels through the hippo pathway in axon pathfinding, suggesting a conserved interaction of NF2 and Slit2 in regulating migration.

Introduction

A critical process in nervous system development is the directed migration of neurons to precise destinations. Directed migration is a complex process that requires integration of extracellular cues into cytoskeletal changes which guide the cell to a specific location. In *C. elegans* the Q neuroblasts are an established system to study directed cell migrations (MIDDELKOOP AND KORSWAGEN 2014). The QR and QL neuroblasts are born in the posterior region of the worm yet migrate in opposite directions (SULSTON AND HORVITZ 1977; SALSER AND KENYON 1992; SALSER *et al.* 1993). QL is born on the left side of the animal and migrates posteriorly over the seam cell V5 before dividing. During this initial migration QL detects a posteriorly derived EGL-20/Wnt signal which through canonical Wnt signaling initiates transcription of *mab-5/Hox* (SALSER AND KENYON 1992). MAB-5 drives further posterior migration of the QL lineage, resulting in the QL.a descendant PQR migrating to the tail near the anus and posterior phasmid ganglion. QR is born on the right side of the animal and migrates anteriorly over the seam cell V4 and away from the EGL-20/Wnt signal (SALSER *et al.* 1993; HARRIS *et al.* 1996; SALSER AND KENYON 1996). QR does not initiate *mab-5* expression in response to Wnt and continues to migrate anteriorly. After division, QR.a undergoes an identical pattern of cell divisions and cell death as QL.a while migrating anteriorly, with AQR completing migration near the posterior pharyngeal bulb in the head (Figure 1)(MALOOF *et al.* 1999; WHANGBO AND KENYON 1999). Initial Q migrations are controlled autonomously by the receptor molecules UNC-40/DCC and PTP-3/LAR (HONIGBERG AND KENYON 2000; SUNDARARAJAN AND LUNDQUIST 2012) and non-autonomously by the Fat-like cadherin CDH-4 (SUNDARARAJAN *et al.* 2014). Later Q

descendant migrations are controlled by Wnt signaling (WHANGBO AND KENYON 1999; ZINOVYEVA AND FORRESTER 2005; ZINOVYEVA *et al.* 2008; HARTERINK *et al.* 2011), which appears to not be involved in initial migration (JOSEPHSON *et al.* 2016), and by the transmembrane receptor MIG-13 in parallel with SDN-1/Syndecan (WANG *et al.* 2013; SUNDARARAJAN *et al.* 2015).

To identify additional molecules that regulate Q migrations, a forward genetic screen for mutations affecting AQR and PQR migration was previously performed. Here we report that this screen identified an allele of *nfm-1*, which encodes a *C. elegans* Neurofibromatosis Type II (NF2)/Merlin molecule. *NF2* acts as a tumor suppressor in humans, and mutations in the gene lead to development of neurofibromatosis type II (GUSELLA *et al.* 1996; GUTMANN *et al.* 1997), a disease of benign Schwannomas that must be removed surgically. NF2/Merlin is involved in signaling pathways involving hippo, mTOR and PI3K-Akt (ZHAO *et al.* 2007; STRIEDINGER *et al.* 2008; JAMES *et al.* 2009; OKADA *et al.* 2009). Additionally, NF2 is involved in nervous system maintenance, corpus callosum development, and axon guidance (SCHULZ *et al.* 2013; LAVADO *et al.* 2014; SCHULZ *et al.* 2014). In corpus callosum development, NF2 inhibits the hippo pathway component Yap. In *NF2* mutants, this inhibition is relieved, resulting in increased expression of *Slit2*, a secreted axon guidance cue that prevents midline crossing. This leads to defects in midline crossing of axons in the callosum (LAVADO *et al.* 2014).

In *C. elegans,* RNAi against *nfm-1* results in embryonic lethality (SKOP *et al.* 2004), and an *nfm-1::gfp* transgene is reported as being localized to the basolateral region of gut epithelium (ZHANG *et al.* 2011). Here we report that two likely hypomorphic

mutations in *nfm-1* display AQR and PQR migration defects. Mosaic analysis and expression studies indicated that NFM-1 might not act in the Q cells themselves (i.e. that it acts non-autonomously). Finally, we show a genetic interaction between NFM-1 and the secreted guidance cue SLT-1 in AQR migration. In vertebrates, Slit1 and Slit2 are required for guidance of many axons, acting through the Robo family receptors (NGUYEN BA-CHARVET *et al.* 1999; PIPER *et al.* 2000; BAGRI *et al.* 2002; UNNI *et al.* 2012; KIM *et al.* 2014). The Slit-Robo guidance pathway is conserved in *C. elegans* where SLT-1 acts as a guidance cue for several neurons through SAX-3/Robo (HAO *et al.* 2001; CHANG *et al.* 2006; QUINN *et al.* 2006; XU AND QUINN 2012). In general, detection of extracellular guidance cues such as *Slit* cause cytoskeletal changes that result in directed migration of cells and axonal growth cones, most typically repulsion. We show that *slt-1* mutations enhance AQR migration defects of *nfm-1* mutations, and that *sax-3* mutants display defects in AQR and PQR migration. These results are consistent with a model in which NFM-1 regulates AQR and PQR migration by controlling the production of an extracellular cue, either SLT-1 itself or an unidentified cue that acts in parallel to SLT-1.

Materials and Methods

Nematode Strains and genetics

C. elegans were grown under standard conditions at 20°C on Nematode Growth Media (NGM) plates (SULSTON AND BRENNER 1974). N2 Bristol was the wild-type strain. Alleles used include LG III: *nfm-1(ok754), nfm-1(lq132),* LG X: *sax-3(ky123), slt-1(ok255), slt-1(eh15).* Standard gonadal injection was used to create the following extrachromosomal arrays: *lqEx773*[*nfm-1::gfp* fosmid (5ng/µL), *Pgcy::32::yfp* (50ng/µL)], *lqEx782* [*Pnfm-1::gfp* (10ng/µL), *Pgcy-32::cfp* (25ng/µL)]. Ultraviolet Trimethylpsoralen (UV/TMP) techniques (MELLO AND FIRE 1995) were used to integrate extrachromosomal arrays to generate the following transgenes: LGII: *lqIs244* [*lqEx737, Pgcy-32::cfp* (25ng/µL)], unknown chromosomal location *lqIs247* [*lqEx773, nfm-1::gfp*], *lqIs274* [*lqEx834, Pegl-17::myr-mCherry* (20ng/µL) *Pegl-l7::mCherry::his-24* (20ng/µL)]. The *nfm-1::gfp* fosmid was obtained from the TransgeneOme project, clone 7039520022144752 D02 (SAROV *et al.* 2006). *nfm-1(ok754)* was maintained as a heterozygote over the *hT2* balancer because homozygous *ok754* animals arrest during larval stages, but positions of AQR and PQR could be scored in these arrested animals. Genotypes with M+ had maternal contribution from the *hT2* balancer.

Scoring migration of AQR and PQR

AQR migrates to a position near post-deirid ganglia in the region of the posterior pharyngeal bulb, and PQR migrates posteriorly to a position near the phasmid ganglia posterior to the anus. We used a method as described previously to score AQR and PQR position using *Pgcy-32* to drive expression of fluorescent proteins (SHAKIR *et al.* 2006;

CHAPMAN *et al.* 2008). Five positions in the anterior-posterior axis of the animal were used to score AQR and PQR position. Position 1 was the wild-type position of AQR and is the region around the posterior pharyngeal bulb. Neurons anterior to the posterior pharyngeal bulb were not observed. Position 2 was posterior to position 1, but anterior to the vulva. Position 3 was the region around the vulva, position 4 was the birthplace of Q cells, and position 5 was posterior to the anus, the wild-type position of PQR (see Figure 2D). A Leica DM550 equipped with YFP, CFP, GFP, and mCherry filters, was used to acquire all micrographs, and for visualization of A/PQR for scoring. Micrographs were acquired using a Qimaging Retiga camera. Significances of difference were determined using Fisher's Exact test.

Mosaic analysis.

Mosaic analysis was conducted as previously described (CHAPMAN *et al.* 2008; SUNDARARAJAN *et al.* 2014). A rescuing *nfm-1(+)* extrachromosomal array was generated using the *nfm-1::gfp* fosmid with a *Pgcy-32::yfp* marker. This array was crossed into *nfm-1(ok754)/hT2; lqIs58 (Pgcy-32::cfp)* to create the rescuing array *lqEx773,* referred to as *nfm-1(+).* Presence of the rescuing array was determined by *Pgcy-32::yfp* expression, and position of AQR and PQR was determined by *Pgcy-32::cfp* expression. *nfm-1(ok754)III; nfm-1(+)* animals were viable and fertile and had wild-type AQR and PQR position, indicating rescue of *nfm-1(ok754)*. Presence of YFP in AQR or PQR indicated *nfm-1(+)* was present in those cells during their migrations. *Pgcy-32* is also expressed in URX, and presence of YFP in the URX neurons indicates other tissues have inherited *nfm-1(+).* Animals that lost *nfm-1(+)* in AQR or PQR, and retained *nfm-*

1(+) in the other Q descendant (PQR and AQR respectively) and URX were scored for AQR and PQR position.

Synchronization of L1 larvae for expression analysis.

L1 Animals carrying *Pnfm-1::gfp* or *nfm-1::gfp* fosmid were synchronized as described previously to the time of Q cell migration (3-5h post hatching)(CHAPMAN *et al.* 2008; SUNDARARAJAN AND LUNDQUIST 2012). Gravid adults were allowed to lay eggs overnight. Plates were washed with M9 buffer, and eggs remained attached to plate. Hatched larvae were collected every half hour using M9 washes and placed onto clean NGM plates for later imaging. *Pegl-17::mCherry* was used as a Q cell marker to determine overlapping expression of *nfm-1* expression constructs.

Results

nfm-1 mutants have defective AQR and PQR migration.

QL and QR undergo identical patterns of cell division, cell death, and neuronal differentiation, but migrate in opposite directions (Figure 1). To identify genes required for AQR and PQR migration, a forward genetic screen using the mutagen ethyl methanesulfonate (EMS) was conducted (SULSTON AND HODGKIN 1988). This screen identified a new mutation with defective AQR and PQR migration, *lq132* (10% AQR defects and 6% PQR defects, Figure 2). The genome of the *lq132*-bearing strain was sequenced and variants were detected using Cloudmap (MINEVICH *et al.* 2012). The strain contained a contained a splice-donor mutation after the fifth exon in the *nfm-1* gene (Figure 2A) (GTATGTGT to ATATGTGT). We scored AQR and PQR migration in the *nfm-1(ok754)* mutant generated by the *C. elegans* gene knock-out consortium. *nfm-1(ok754)* is an in-frame 1042-bp deletion with breakpoints in exons 3 and 7 that removes all of exons 4, 5, and 6 (Figure 2A and B). *nfm-1(ok754)* homozygotes arrested as larvae, but we were able to score AQR and PQR position in arrested larvae. *nfm-1(ok754)* had strong AQR defects, with 88% of AQR failing to migrate to the head, and occasional (1%) posterior AQR migration (Figure 2C and E). *nfm-1(ok754)* also had significant PQR defects, with 15% of PQR failing to migrate into the wild-type position 5 posterior to the anus (Figure 2F). An *nfm-1::gfp* fosmid transgene rescued AQR and PQR defects of both *lq132* and *ok754*, indicating that mutations in *nfm-1* were causative for the migration deficiencies of *lq132* and *ok754* (Figure 2E and F).

nfm-1 encodes a protein similar to human NF2/Merlin (43% identity), and contains Four-Point-One Ezrin Radixin and Moesin (FERM) N, B, and C domains at the

N-terminus (Figure 2B). The *lq132* splice donor mutation occurred after the conserved FERM domain regions, and the *ok754* in-frame deletion removes the entire FERM C domain, including the putative actin-binding site (Figure 2B). RNAi of *nfm-1* caused embryonic lethality (SKOP *et al.* 2004). Thus, both *lq132* and *ok754* are likely not null alleles and retain some function. AQR migration defects in *ok754* were significantly strong than *lq132*, suggesting that *ok754* is a stronger allele than *lq132*.

Mosaic analysis indicates a non-autonomous requirement for *nfm-1* in anterior AQR migration

Genetic mosaic analysis using a rescuing *nfm-1(+)* extrachromosomal array was used to test if *nfm-1* was required in the Q cells themselves (see Methods). In *C. elegans,* extrachromosomal arrays are not stably inherited meiotically, and can be lost during mitotic cell divisions, creating genetically mosaic animals. We used an established strategy to score mosaic animals that had lost an *nfm-1(+)* rescuing transgene in AQR or PQR lineage (see Methods and (CHAPMAN *et al.* 2008; SUNDARARAJAN *et al.* 2014)). This strategy uses a stable *Pgcy-32::cfp* integrated transgene to visualize AQR and PQR in all animals, and an unstable array *nfm-1(+),* carrying the rescuing *nfm-1::gfp* fosmid and *Pgcy-32::yfp* (Figure 4.3). Non-mosaic *nfm-1(ok754)* animals that harbored the *nfm-1(+)* array were viable, fertile, and were rescued for AQR and PQR migration (Figure 2E and F). We analyzed 89 mosaic animals in which the *nfm-1(+)* array was lost from the AQR lineage, but retained in PQR and URX lineages as shown in Figure 3. These animals were rescued for AQR migration defects despite loss of *nfm-1(+)* in AQR, suggesting that *nfm-1* is required non-autonomously for anterior AQR migration (Figures

198 3B and C and 4A). Similarly, PQR migration defects were still rescued in 75 mosaic
199 animals in which PQR that had lost the *nfm-1(+)* array (Figure 4B). Animals mosaic for
200 *nfm-1(+)* in AQR or PQR rescued *nfm-1(ok754)* defects to a similar level as non-mosaics
201 (*nfm-1(+)* in AQR and PQR) (Figure 4A and B). In sum, this mosaic analysis indicates
202 that *nfm-1* function was not required in AQR and PQR for their proper migration, and
203 that *nfm-1* might act non-autonomously in this process.
204 Using this method, it was impossible to determine which tissues require *nfm-1*.
205 Based on cell lineages (Figure 3A), presence of *nfm-1(+)* array in URX and either AQR
206 or PQR suggests it is present broadly in AB-derived lineages. P lineages were not
207 assayed in this study, but mosaic *nfm-1(ok754)* animals, which normally arrest as sterile
208 larvae, grew to viable and fertile adults, again suggesting broad *nfm-1* distribution in the
209 mosaics, possibly including P-derived germ line and gonad lineages. It is possible that
210 perdurance of NFM-1 protein, or array loss in the Q lineages themselves led to *nfm-1*
211 function in the Q lineages despite loss in AQR or PQR. To account for these rare but
212 possible events, we scored at least 70 mosaic animals. Overall, mosaic analysis suggests
213 that *nfm-1* acts non-autonomously in AQR and PQR migration, as loss of the rescuing
214 array in AQR or PQR did not correlate with mutant phenotype.
215
216 ***nfm-1::gfp* transcriptional and translational reporter expression was not apparent**
217 **in Q lineages.**
218 A *Pnfm-1::gfp* transcriptional reporter was created by using a 2.1-kb region
219 upstream of *nfm-1* to drive expression of GFP. This 2.1-kb region was the entire upstream
220 region between *nfm-1* and the next gene *anmt-2.* At the time of Q migration, this

construct showed expression in posterior cells near the anus, including posterior intestinal cells, the three rectal gland cells, and other unidentified cells that might be the anal sphincter muscle and the stomatointestinal muscle (Figure 5A-C). Variable expression in the hypodermis was also observed (Figure 5 A-C). Overlap between *Pnfm-1::gfp* and *Pegl-17::mCherry*, a Q cell marker, was not observed, consistent with *nfm-1* not being expressed in the Q neuroblasts during their migrations (Figure 5A-C). Likewise, full length NFM-1::GFP expression from the rescuing fosmid was not observed in migrating Q cells (Figure 6). NFM-1::GFP was detected in the posterior gut region. In sum, no *nfm-1* transgene expression was observed in the Q cells during their migration.

slt-1 mutations enhance AQR defects of _nfm-1(lq132)_.

Previous studies suggested that *NF2* can non-autonomously affect axon guidance in the developing mouse brain (LAVADO *et al.* 2014). This guidance mechanism occurs through regulation of *Slit2* mRNA levels, suggesting a transcriptional role of *NF2* (LAVADO *et al.* 2014). *Slit2* is a secreted guidance cue for developing neurons, and is detected by the Robo receptor. Because of interactions between *Slit2* and *NF2* we investigated the interaction of *nfm-1* and the *C. elegans Slit2* homolog *slt-1* in Q descendant migration. In this study we used one null allele *slt-1(eh15),* and one strong loss-of-function in frame deletion allele *slt-1(ok255)* (HAO *et al.* 2001; STEIMEL *et al.* 2013). *slt-1* mutations had no effect on AQR and PQR migration on their own, but enhanced AQR migration defects of *nfm-1(lq132)* and *nfm-1(ok754)* (Figure 7). *slt-1* had no effect on PQR migration in double mutants. We tested the SLT-1 receptor SAX-3/Robo, and *sax-3(ky123)* mutants

243 showed weak but significant defects in both AQR and PQR migration, consistent with

244 SAX-3 promoting migration of the Q lineages (Figure 7).

245

Discussion

The NF2/Merlin molecule NFM-1 promotes migration of AQR and PQR.

Complete migration of the QR and QL descendants AQR and PQR requires the coordination of many genes (MIDDELKOOP AND KORSWAGEN 2014). Although numerous molecules have been identified that act in the Q cells to promote migration, such as the transmembrane receptors UNC-40/DCC, PTP-3/LAR, and MIG-13 (SUNDARARAJAN AND LUNDQUIST 2012; WANG *et al.* 2013; SUNDARARAJAN *et al.* 2015), fewer have been identified that act outside the Q cells to control their migration. Of the non-autonomous genes that have been implicated in Q descendant migration, most are secreted molecules such as Wnts (HUNTER *et al.* 1999; WHANGBO AND KENYON 1999; KORSWAGEN 2002; PAN *et al.* 2006), although some transmembrane genes such as CDH-4 have been demonstrated to non-autonomously affect Q cell migration (SUNDARARAJAN *et al.* 2014).

Here we present data identifying a non-autonomous role for the FERM domain-containing molecule NFM-1 in promoting Q migration. NFM-1 is similar to human NF2/Merlin, the molecule affected in Neurofibromatosis type II. We found that mutations in *nfm-1* resulted in severe AQR migration defects, and to a lesser extent PQR migration defects. These defects typically manifested as incomplete migrations, suggesting that these *nfm-1* mutations did not affect direction of migration along the anterior/posterior axis, but rather the migratory capacity of these cells.

Loss of *NF2/Merlin* function in either mouse or *Drosophila* results in embryonic lethality (FEHON *et al.* 1997; MCCLATCHEY *et al.* 1997). In *C. elegans, nfm-1* appears to be required in embryonic development similar to other animals, as RNAi against *nfm-1* is reported as embryonic lethal (SKOP *et al.* 2004), and no null alleles of *nfm-1* have been

described. The two *nfm-1* mutations studied here are not complete loss of function and likely retain some NFM-1 function. The 5' splice site mutant *nfm-1(lq132)* was viable and fertile, and the in-frame deletion allele *nfm-1(ok754)* caused larval arrest. It is possible that complete loss of *nfm-1* function results in more severe AQR and PQR migration defects, possibly even directional defects, not observed in these alleles. The *nfm-1(ok754*) in-frame deletion removes part of the FERMB domain and the entire FERMC domain, suggesting that these domains are important in AQR and PQR migration.

NFM-1 acts non-autonomously in AQR and PQR migration.

As a cytoskeletal-membrane linker with a potential actin-binding domain, we hypothesized that NFM-1 might regulate actin-based membrane protrusion in migrating cells. However, a genetic mosaic analysis indicated that NFM-1 was not required in AQR or PQR for their migration. Furthermore, expression of transgenes of the *nfm-1* promoter and a rescuing full-length *nfm-1::gfp* were not observed in Q lineages. Rather, expression was observed in in posterior region near the anus, including posterior intestine, the rectal gland cells and potentially the anal sphincter muscle and stomatointestinal muscle. While the mosaic analysis was unable to discern the tissue in which NFM-1 acts, these expression studies suggest that NFM-1 function in the posterior region of the gut near the anus might regulate AQR and PQR migration. However, hypodermal expression is also a possibility. In sum, mosaic analysis and expression studies indicate that NFM-1 acts outside of the AQR and PQR, non-autonomously, to regulate their migration.

nfm-1 and _slt-1_ interact genetically to promote anterior AQR migration.

In *Drosophila* and mice, *NF2/Merlin* is known to regulate several signaling pathways, including stimulating the Hippo pathway to inhibit the Yorkie transcription cofactor (HAMARATOGLU *et al.* 2006; MOROISHI *et al.* 2015). In mice, loss of *NF2* in neural progenitor cells results in upregulation of Yap (LAVADO *et al.* 2014). High Yap activity leads to ectopic levels of the secreted guidance cue *Slit2* which causes defects in midline axon guidance (LAVADO *et al.* 2014). Interestingly, this is a non-autonomous role of *NF2* in midline axon guidance, similar to our observation of *nfm-1* in *C. elegans* neuronal migration. The Hippo pathway in *C. elegans* is poorly conserved, and the *C. elegans* genome does not encode a clear Yap homolog (HILMAN AND GAT 2011). We tested the role of the single *C. elegans Slit* gene *slt-1* in AQR/PQR migration and interaction with *nfm-1*. *slt-1* regulates the anterior-posterior migration of the CAN neurons in embryos (HAO *et al.* 2001). Although no migration defects were detected in *slt-1* mutants alone, they did enhance AQR migration defects of *nfm-1(lq132)* and *nfm-1(ok754)*. This enhancement is consistent with NFM-1 and SLT-1 acting in parallel pathways, but since we do not know the null phenotype of NFM-1 with regard to AQR and PQR, the possibility that they act in the same pathway cannot be excluded.

Interestingly no enhancement of *nfm-1* PQR migration defects was seen in *slt-1; nfm-1* double mutants. This suggests that *slt-1* and *nfm-1* interact in AQR migration but not PQR migration. This is of note because *nfm-1* is expressed in posterior tissues where PQR migrates, and away from which AQR migrates. *sax-3/Robo* mutants displayed both AQR and PQR migration defects. Possibly, SAX-3/Robo acts with SLT-1 in AQR migration, and with an unidentified ligand in PQR migration. In mice, midline axon

316 defects are due to excess Slit2 expression in *NF2* mutants. The phenotypic enhancement
317 that we observe between *slt-1* and *nfm-1* suggests that these molecules are both required
318 for AQR migration. Further studies of the interaction between *nfm-1* and *slt-1* will be
319 required to understand the role of these molecules in AQR migration.

320 Our results, combined with those in vertebrates, are consistent with the idea that
321 NFM-1 promotes the production of a signal or signals that regulate AQR and PQR
322 migration. This could be SLT-1 itself, such as in vertebrates, or a molecule that acts in
323 parallel to SLT-1. The *slt-1* expression pattern is dynamic throughout development, but
324 *slt-1* is expressed in posterior cells including body wall muscles and the anal sphincter
325 muscle (HAO *et al.* 2001). Whether *nfm-1* can control pathways that regulate transcription
326 as it does in vertebrates, or maintains epidermal integrity to control migration, is unclear,
327 but our studies suggest that NFM-1 interacts with cues that guide AQR and PQR
328 migrations.

Acknowledgments

The authors thank members of the Lundquist and Ackley labs for discussion, and E. Struckhoff for technical assistance. Some *C. elegans* strains were provided by the CGC, which is funded by NIH Office of Research Infrastructure Programs (P40 OD010440). Some next-generation sequencing was provided by the University of Kansas Genome Sequencing Core Laboratory of the Center for Molecular Analysis of Disease Pathways (NIH P20 GM103638). This work was supported by NIH grants R01 NS040945 and R21 NS070417 to E.A.L., and the Kansas Infrastructure Network of Biomedical Research Excellence (NIH P20 GM103418). M.P.J was supported by the Madison and Lila Self Graduate Fellowship at the University of Kansas, and R.A. was a KINBRE Undergraduate Research Scholar (NIH P20 GM103418).

340 **Figure 1. Migration of QR and QL descendants.** A-B) Diagrams representing the
341 migration and cell division pattern of QR on the right side (A) and QL on the left side (B)
342 in the L1 animal, showing birthplace of the Q neuroblasts, and approximate locations of
343 the Q descendants. Maroon shading represents the posteriorly derived EGL-20/Wnt
344 signal. White ovals are hypodermal seam cells V1-V6. Circles with black x indicate cells
345 that undergo programmed cell death after cell division. Dorsal is up, anterior to the left.
346 C) Merged DIC and fluorescent micrograph showing location of Q descendants AQR and
347 PQR in an adult wild-type animal. *Pgcy-32::cfp* is expressed in AQR, PQR and URXL/R.
348 The scale bar represents 10μM.
349
350 **Figure 2. Position of Q descendants AQR and PQR in *nfm-1* mutants.** A) A diagram
351 of the *nfm-1* locus and alleles used. The *ok754* deletion (dashed line), and *lq132* splice
352 site mutation (arrow) are noted. B) NFM-1 isoform A domain structure and allele
353 locations are shown. The FERM domain lobes N (gray), B (black), and C (white) are
354 shown. The black bar under FERM C represents predicted actin-binding motif. The
355 dashed line is *ok754* in frame deletion, and *lq132* splice donor mutation location is
356 marked by an arrow. C) Merged DIC and fluorescent micrograph of an *nfm-1(ok754)*
357 arrested larval mutant animal. Both AQR and PQR failed to migrate (PQR wild-type
358 position noted by arrowhead). Scale bar represents 10μM. D) Diagram of scoring
359 positions in an L4 animal, with wild-type locations of AQR and PQR shown as magenta
360 circles. E-F) Chart showing percent of AQR (E) or PQR (F) in positions 1-5 in different
361 genotypes. All animals unless otherwise noted were scored using *lqIs58 (Pgcy-32::cfp)*.
362 M+ indicates animals were scored from heterozygous mother and have wild-type

363 maternal contribution of *nfm-1*. *nfm-1(+)* animals harbor the array containing the *nfm-*
364 *1::gfp* fosmid. Asterisks indicate significant) difference from wild-type (N>100 *$p<0.05$,
365 **$p<0.005$, ***$p<0.0005$ Fisher's exact test). Pound signs indicate, for that position, a
366 significant rescue of corresponding *nfm-1* mutant (N>100 #$p<0.05$, ##$p<0.005$,
367 ###$p<0.0005$, Fisher's exact test). Error bars represent two times the standard error of the
368 proportion.
369
370 **Figure 3. *nfm-1* mosaic analysis.** A) The abbreviated lineage of cells that express *Pgcy-*
371 *32* (red). Numbers next to lines indicate the number of cell divisions not shown. The X
372 next to AQR and PQR indicates the sister of A/PQR (QL/R.aa) that undergoes
373 programmed cell death. B) Fluorescent micrograph taken with CFP filter of *nfm-*
374 *1(ok754); nfm-1(+), Pgcy-32::cfp* mosaic animal with correct placement of AQR and
375 PQR. C) Fluorescent micrograph of the same animal from B using a YFP filter. AQR is
376 not visible in this animal indicating that somewhere in AQR lineage, the *nfm-1(+)*
377 transgene was lost. YFP is detected in URXL/R, and PQR indicating many tissues
378 retained *nfm-1(+)*. Scale bar represent 10μM.
379
380 **Figure 4. Analysis of *nfm-1(+)* mosaic animals.** Quantification of AQR (A), and PQR
381 (B) migration as in Figure 2, with *nfm-1(+)* mosaic animals. *nfm-1(+)* represents
382 presence of *nfm-1* rescuing fosmid. *nfm-1(+)* rescued *ok754* lethality, and animals were
383 maintained as rescued homozygous *ok754* mutants. Mosaic animals have *nfm-1(+)* in
384 URX but have lost *nfm-1(+)* in either AQR or PQR. Pound signs indicate, for that
385 position, a significant rescue of corresponding *nfm-1* mutant (N>100 #$p<0.05$,

386 ##$p<0.005$, ###$p<0.0005$, Fisher's exact test). Error bars represent two times the standard
387 error of the proportion.
388
389 **Figure 5. *nfm-1* transcriptional reporter was not expressed in Q cells during their**
390 **early migrations.** A-C) Ventral view of the posterior region of a *Pnfm-1::gfp; Pegl-*
391 *17::mCherry* transgenic animal staged to 3-3.5h post hatching. A) A GFP Micrograph
392 showing expression of *Pnfm-1::gfp*. Expression was seen in posterior cells near the anus,
393 including posterior intestinal cells (Int) the three rectal gland cells (Rect). Other
394 unidentified cells in the region were possibly the anal sphincter muscle and the
395 stomatointestinal muscle. Variable hypodermal expression was observed along the length
396 of the animal (Hyp). B) An mCherry micrograph shows Q cell specific expression during
397 their migrations. C) Merged. GFP is not observed in Q cells, but is expressed in
398 neighboring tissues and posterior cells. Scale bar is 10μm, anterior is to the left, right is
399 up.
400
401 **Figure 6. *nfm-1::gfp* translational reporter was excluded from Q cells.** A-C) Lateral
402 view of a staged 3-3-5h post hatching L1 *nfm-1::gfp; Pegl-17::mCherry* animal. A)
403 Fluorescent micrograph of GFP expression from *nfm-1::gfp* rescuing fosmid. Asterisk
404 marks URX expression of *Pgcy-32::yfp* in the head that was not excluded by GFP filter.
405 The dashed rectangle indicates the enlarged posterior section in D-F. B) *Pegl-*
406 *17::mCherry*, fluorescent micrograph showing location of early Q neuroblasts. QL is out
407 of focus because QL and QR are on different planes, QR on the right side, and QL on left
408 side of the animal. C) Merge of A and B. No overlap of mCherry and GFP was observed.

409 D-F) Enlarged posterior section of A-C. Anterior is left, dorsal is up. D) Enlargement of
410 A to show *nfm-1::gfp* present in posterior region near the anus. E) Enlargement of B. QL
411 is outlined to distinguish it from the V5 seam cell that transiently expresses *Pegl-17*. F)
412 Enlargement of C. Scale bars in C and F represent 10 μm.
413
414 **Figure 7. *slt-1* enhances *nfm-1* AQR migration defects.** A) Percentage of AQR in each
415 position, quantified as in Figure 2. B) PQR migration. Asterisks indicate significant
416 difference from wild-type (N>100 *$p<0.05$, **$p<0.005$, ***$p<0.0005$ Fisher's exact
417 test). Pound signs indicate, for that position, a significant enhancement of the
418 corresponding *nfm-1* mutant (N>100 #$p<0.05$, ##$p<0.005$, ###$p<0.0005$, Fisher's exact
419 test). Error bars represent two times the standard error of the proportion.

References

Bagri, A., O. Marin, A. S. Plump, J. Mak, S. J. Pleasure *et al.*, 2002 Slit proteins prevent midline crossing and determine the dorsoventral position of major axonal pathways in the mammalian forebrain. Neuron 33**:** 233-248.

Chang, C., C. E. Adler, M. Krause, S. G. Clark, F. B. Gertler *et al.*, 2006 MIG-10/lamellipodin and AGE-1/PI3K promote axon guidance and outgrowth in response to slit and netrin. Curr Biol 16**:** 854-862.

Chapman, J. O., H. Li and E. A. Lundquist, 2008 The MIG-15 NIK kinase acts cell-autonomously in neuroblast polarization and migration in C. elegans. Dev Biol 324**:** 245-257.

Fehon, R. G., T. Oren, D. R. LaJeunesse, T. E. Melby and B. M. McCartney, 1997 Isolation of mutations in the Drosophila homologues of the human Neurofibromatosis 2 and yeast CDC42 genes using a simple and efficient reverse-genetic method. Genetics 146**:** 245-252.

Gusella, J. F., V. Ramesh, M. MacCollin and L. B. Jacoby, 1996 Neurofibromatosis 2: loss of merlin's protective spell. Curr Opin Genet Dev 6**:** 87-92.

Gutmann, D. H., M. J. Giordano, A. S. Fishback and A. Guha, 1997 Loss of merlin expression in sporadic meningiomas, ependymomas and schwannomas. Neurology 49**:** 267-270.

Hamaratoglu, F., M. Willecke, M. Kango-Singh, R. Nolo, E. Hyun *et al.*, 2006 The tumour-suppressor genes NF2/Merlin and Expanded act through Hippo signalling to regulate cell proliferation and apoptosis. Nat Cell Biol 8**:** 27-36.

Hao, J. C., T. W. Yu, K. Fujisawa, J. G. Culotti, K. Gengyo-Ando *et al.*, 2001 C. elegans slit acts in midline, dorsal-ventral, and anterior-posterior guidance via the SAX-3/Robo receptor. Neuron 32**:** 25-38.

Harris, J., L. Honigberg, N. Robinson and C. Kenyon, 1996 Neuronal cell migration in C. elegans: regulation of Hox gene expression and cell position. Development 122**:** 3117-3131.

Harterink, M., D. H. Kim, T. C. Middelkoop, T. D. Doan, A. van Oudenaarden *et al.*, 2011 Neuroblast migration along the anteroposterior axis of C. elegans is controlled by opposing gradients of Wnts and a secreted Frizzled-related protein. Development 138**:** 2915-2924.

Hilman, D., and U. Gat, 2011 The evolutionary history of YAP and the hippo/YAP pathway. Mol Biol Evol 28**:** 2403-2417.

Honigberg, L., and C. Kenyon, 2000 Establishment of left/right asymmetry in neuroblast migration by UNC-40/DCC, UNC-73/Trio and DPY-19 proteins in C. elegans. Development 127**:** 4655-4668.

Hunter, C. P., J. M. Harris, J. N. Maloof and C. Kenyon, 1999 Hox gene expression in a single Caenorhabditis elegans cell is regulated by a caudal homolog and intercellular signals that inhibit wnt signaling. Development 126**:** 805-814.

James, M. F., S. Han, C. Polizzano, S. R. Plotkin, B. D. Manning *et al.*, 2009 NF2/merlin is a novel negative regulator of mTOR complex 1, and activation of mTORC1 is associated with meningioma and schwannoma growth. Mol Cell Biol 29**:** 4250-4261.

464 Josephson, M. P., Y. Chai, G. Ou and E. A. Lundquist, 2016 EGL-20/Wnt and MAB-
465 5/Hox Act Sequentially to Inhibit Anterior Migration of Neuroblasts in C.
466 elegans. PLoS One 11**:** e0148658.
467 Kim, M., W. T. Farmer, B. Bjorke, S. A. McMahon, P. J. Fabre *et al.*, 2014 Pioneer
468 midbrain longitudinal axons navigate using a balance of Netrin attraction and Slit
469 repulsion. Neural Dev 9**:** 17.
470 Korswagen, H. C., 2002 Canonical and non-canonical Wnt signaling pathways in
471 Caenorhabditis elegans: variations on a common signaling theme. Bioessays 24**:**
472 801-810.
473 Lavado, A., M. Ware, J. Pare and X. Cao, 2014 The tumor suppressor Nf2 regulates
474 corpus callosum development by inhibiting the transcriptional coactivator Yap.
475 Development 141**:** 4182-4193.
476 Maloof, J. N., J. Whangbo, J. M. Harris, G. D. Jongeward and C. Kenyon, 1999 A Wnt
477 signaling pathway controls hox gene expression and neuroblast migration in C.
478 elegans. Development 126**:** 37-49.
479 McClatchey, A. I., I. Saotome, V. Ramesh, J. F. Gusella and T. Jacks, 1997 The Nf2
480 tumor suppressor gene product is essential for extraembryonic development
481 immediately prior to gastrulation. Genes Dev 11**:** 1253-1265.
482 Mello, C., and A. Fire, 1995 DNA transformation. Methods Cell Biol 48**:** 451-482.
483 Middelkoop, T. C., and H. C. Korswagen, 2014 Development and migration of the C.
484 elegans Q neuroblasts and their descendants. WormBook**:** 1-23.
485 Minevich, G., D. S. Park, D. Blankenberg, R. J. Poole and O. Hobert, 2012 CloudMap: a
486 cloud-based pipeline for analysis of mutant genome sequences. Genetics 192**:**
487 1249-1269.
488 Moroishi, T., H. W. Park, B. Qin, Q. Chen, Z. Meng *et al.*, 2015 A YAP/TAZ-induced
489 feedback mechanism regulates Hippo pathway homeostasis. Genes Dev 29**:** 1271-
490 1284.
491 Nguyen Ba-Charvet, K. T., K. Brose, V. Marillat, T. Kidd, C. S. Goodman *et al.*, 1999
492 Slit2-Mediated chemorepulsion and collapse of developing forebrain axons.
493 Neuron 22**:** 463-473.
494 Okada, M., Y. Wang, S. W. Jang, X. Tang, L. M. Neri *et al.*, 2009 Akt phosphorylation
495 of merlin enhances its binding to phosphatidylinositols and inhibits the tumor-
496 suppressive activities of merlin. Cancer Res 69**:** 4043-4051.
497 Pan, C. L., J. E. Howell, S. G. Clark, M. Hilliard, S. Cordes *et al.*, 2006 Multiple Wnts
498 and frizzled receptors regulate anteriorly directed cell and growth cone migrations
499 in Caenorhabditis elegans. Dev Cell 10**:** 367-377.
500 Piper, M., K. Georgas, T. Yamada and M. Little, 2000 Expression of the vertebrate Slit
501 gene family and their putative receptors, the Robo genes, in the developing
502 murine kidney. Mech Dev 94**:** 213-217.
503 Quinn, C. C., D. S. Pfeil, E. Chen, E. L. Stovall, M. V. Harden *et al.*, 2006 UNC-6/netrin
504 and SLT-1/slit guidance cues orient axon outgrowth mediated by MIG-
505 10/RIAM/lamellipodin. Curr Biol 16**:** 845-853.
506 Salser, S. J., and C. Kenyon, 1992 Activation of a C. elegans Antennapedia homologue in
507 migrating cells controls their direction of migration. Nature 355**:** 255-258.

Salser, S. J., and C. Kenyon, 1996 A C. elegans Hox gene switches on, off, on and off again to regulate proliferation, differentiation and morphogenesis. Development 122**:** 1651-1661.

Salser, S. J., C. M. Loer and C. Kenyon, 1993 Multiple HOM-C gene interactions specify cell fates in the nematode central nervous system. Genes Dev 7**:** 1714-1724.

Sarov, M., S. Schneider, A. Pozniakovski, A. Roguev, S. Ernst *et al.*, 2006 A recombineering pipeline for functional genomics applied to Caenorhabditis elegans. Nat Methods 3**:** 839-844.

Schulz, A., S. L. Baader, M. Niwa-Kawakita, M. J. Jung, R. Bauer *et al.*, 2013 Merlin isoform 2 in neurofibromatosis type 2-associated polyneuropathy. Nat Neurosci 16**:** 426-433.

Schulz, A., A. Zoch and H. Morrison, 2014 A neuronal function of the tumor suppressor protein merlin. Acta Neuropathol Commun 2**:** 82.

Shakir, M. A., J. S. Gill and E. A. Lundquist, 2006 Interactions of UNC-34 Enabled with Rac GTPases and the NIK kinase MIG-15 in Caenorhabditis elegans axon pathfinding and neuronal migration. Genetics 172**:** 893-913.

Skop, A. R., H. Liu, J. Yates, 3rd, B. J. Meyer and R. Heald, 2004 Dissection of the mammalian midbody proteome reveals conserved cytokinesis mechanisms. Science 305**:** 61-66.

Steimel, A., J. Suh, A. Hussainkhel, S. Deheshi, J. M. Grants *et al.*, 2013 The C. elegans CDK8 Mediator module regulates axon guidance decisions in the ventral nerve cord and during dorsal axon navigation. Dev Biol 377**:** 385-398.

Striedinger, K., S. R. VandenBerg, G. S. Baia, M. W. McDermott, D. H. Gutmann *et al.*, 2008 The neurofibromatosis 2 tumor suppressor gene product, merlin, regulates human meningioma cell growth by signaling through YAP. Neoplasia 10**:** 1204-1212.

Sulston, J., and J. Hodgkin, 1988 Methods, pp. 587-606 in *The Nematode Caenorhabditis elegans*, edited by W. B. Wood. Cold Spring Harbor Laboratory Press, Cold Spring Harbor, New York.

Sulston, J. E., and S. Brenner, 1974 The DNA of Caenorhabditis elegans. Genetics 77**:** 95-104.

Sulston, J. E., and H. R. Horvitz, 1977 Post-embryonic cell lineages of the nematode, Caenorhabditis elegans. Dev Biol 56**:** 110-156.

Sundararajan, L., and E. A. Lundquist, 2012 Transmembrane proteins UNC-40/DCC, PTP-3/LAR, and MIG-21 control anterior-posterior neuroblast migration with left-right functional asymmetry in Caenorhabditis elegans. Genetics 192**:** 1373-1388.

Sundararajan, L., M. L. Norris and E. A. Lundquist, 2015 SDN-1/Syndecan Acts in Parallel to the Transmembrane Molecule MIG-13 to Promote Anterior Neuroblast Migration. G3 (Bethesda).

Sundararajan, L., M. L. Norris, S. Schoneich, B. D. Ackley and E. A. Lundquist, 2014 The fat-like cadherin CDH-4 acts cell-non-autonomously in anterior-posterior neuroblast migration. Dev Biol 392**:** 141-152.

Unni, D. K., M. Piper, R. X. Moldrich, I. Gobius, S. Liu *et al.*, 2012 Multiple Slits regulate the development of midline glial populations and the corpus callosum. Dev Biol 365**:** 36-49.

554 Wang, X., F. Zhou, S. Lv, P. Yi, Z. Zhu *et al.*, 2013 Transmembrane protein MIG-13
555 links the Wnt signaling and Hox genes to the cell polarity in neuronal migration.
556 Proc Natl Acad Sci U S A 110**:** 11175-11180.
557 Whangbo, J., and C. Kenyon, 1999 A Wnt signaling system that specifies two patterns of
558 cell migration in C. elegans. Mol Cell 4**:** 851-858.
559 Xu, Y., and C. C. Quinn, 2012 MIG-10 functions with ABI-1 to mediate the UNC-6 and
560 SLT-1 axon guidance signaling pathways. PLoS Genet 8**:** e1003054.
561 Zhang, H., N. Abraham, L. A. Khan, D. H. Hall, J. T. Fleming *et al.*, 2011 Apicobasal
562 domain identities of expanding tubular membranes depend on glycosphingolipid
563 biosynthesis. Nat Cell Biol 13**:** 1189-1201.
564 Zhao, B., X. Wei, W. Li, R. S. Udan, Q. Yang *et al.*, 2007 Inactivation of YAP
565 oncoprotein by the Hippo pathway is involved in cell contact inhibition and tissue
566 growth control. Genes Dev 21**:** 2747-2761.
567 Zinovyeva, A. Y., and W. C. Forrester, 2005 The C. elegans Frizzled CFZ-2 is required
568 for cell migration and interacts with multiple Wnt signaling pathways. Dev Biol
569 285**:** 447-461.
570 Zinovyeva, A. Y., Y. Yamamoto, H. Sawa and W. C. Forrester, 2008 Complex Network
571 of Wnt Signaling Regulates Neuronal Migrations During Caenorhabditis elegans
572 Development. Genetics 179**:** 1357-1371.
573

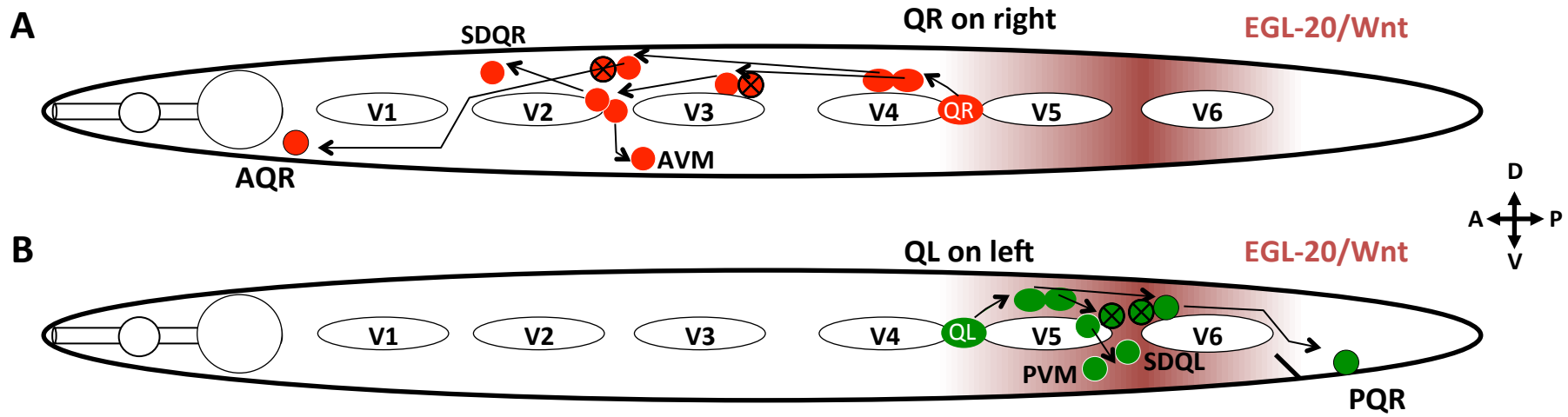
A
QR on right
EGL-20/Wnt
SDQR
V1
V2
V3
V4
QR
V5
V6
AVM
AQR
D
A
P
V
B
QL on left
EGL-20/Wnt
V1
V2
V3
V4
QL
V5
V6
SDQL
PVM
PQR


C
Pgcy-32::cfp
URX L/R
AQR
PQR

Fig. 1

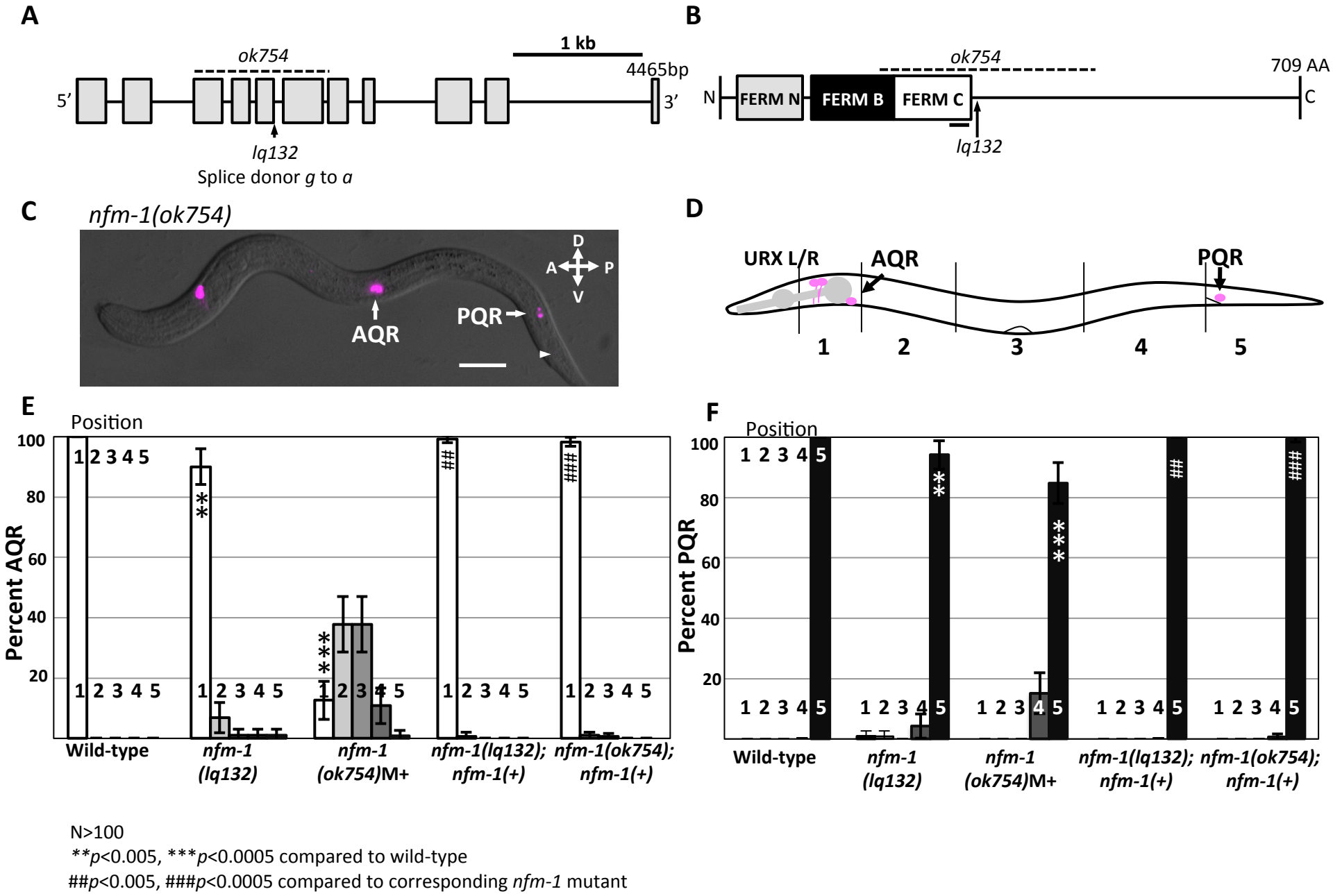

N>100

***p*<0.005, ****p*<0.0005 compared to wild-type

##*p*<0.005, ###*p*<0.0005 compared to corresponding *nfm-1* mutant

Fig. 2

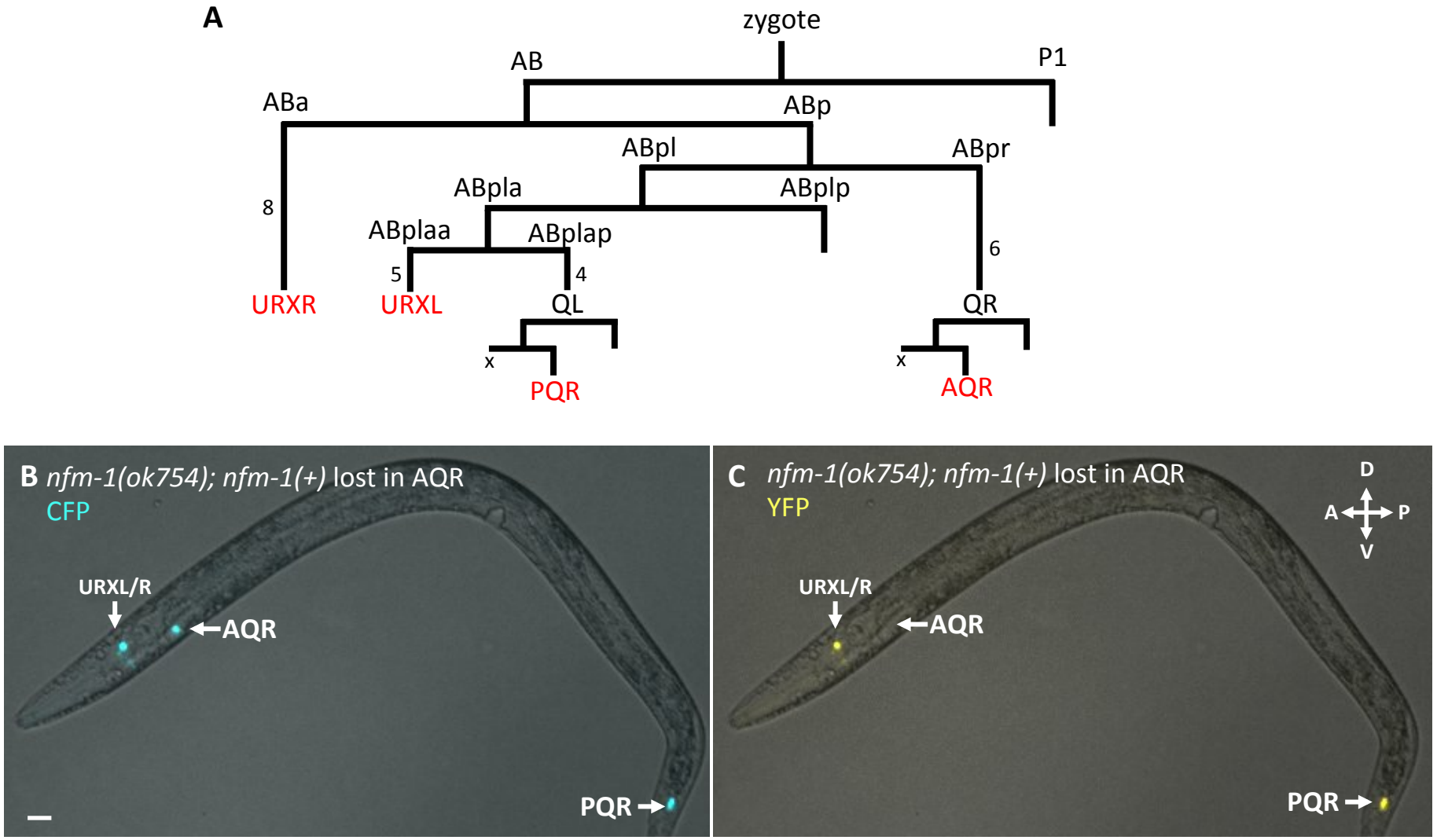
A
zygote
AB
P1
ABa
ABp
ABpl
ABpr
ABpla
ABplp
ABplaa
ABplap
8
5
4
6
URXR
URXL
QL
QR
x
x
PQR
AQR
B nfm-1(ok754); nfm-1(+) lost in AQR
CFP
URXL/R
AQR
PQR
C nfm-1(ok754); nfm-1(+) lost in AQR
YFP
URXL/R
AQR
PQR
D
A
P
V

Fig. 3

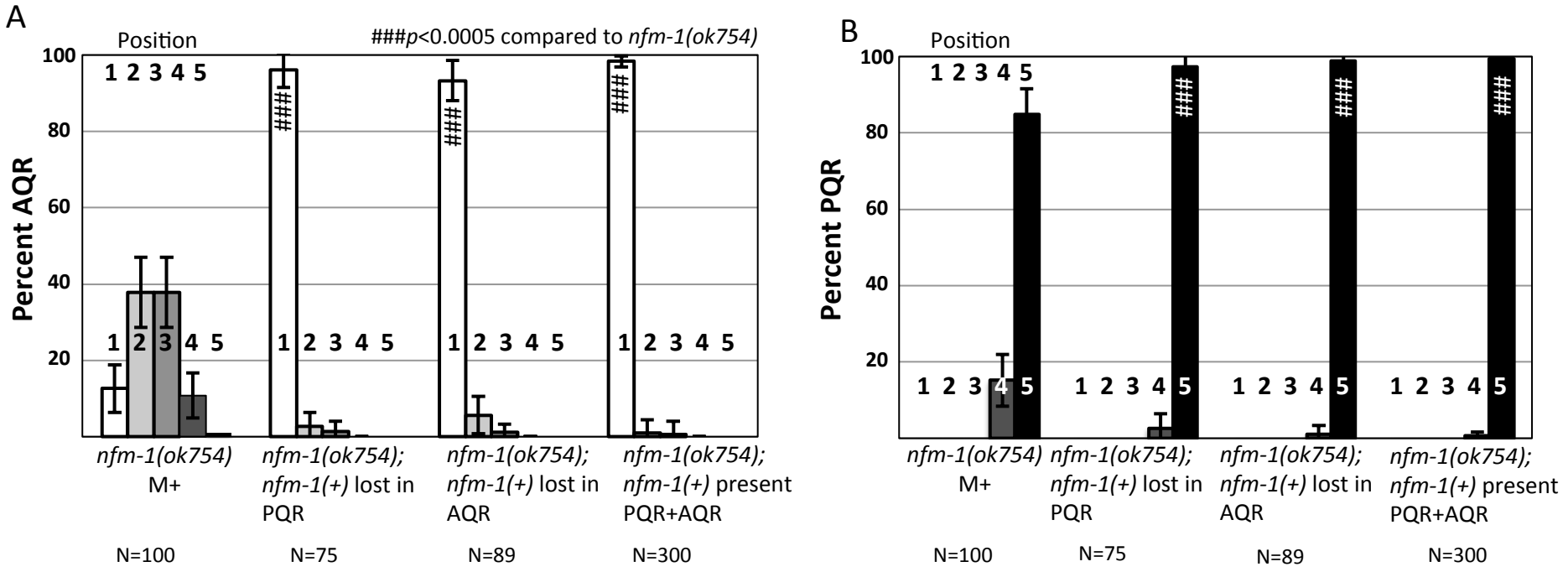
A
Position
###p<0.0005 compared to nfm-1(ok754)
Percent AQR
100
80
60
40
20
1 2 3 4 5
###
nfm-1(ok754) M+
nfm-1(ok754); nfm-1(+) lost in PQR
nfm-1(ok754); nfm-1(+) lost in AQR
nfm-1(ok754); nfm-1(+) present PQR+AQR
N=100
N=75
N=89
N=300
B
Position
Percent PQR
100
80
60
40
20
1 2 3 4 5
###
nfm-1(ok754) M+
nfm-1(ok754); nfm-1(+) lost in PQR
nfm-1(ok754); nfm-1(+) lost in AQR
nfm-1(ok754); nfm-1(+) present PQR+AQR
N=100
N=75
N=89
N=300

Fig. 4

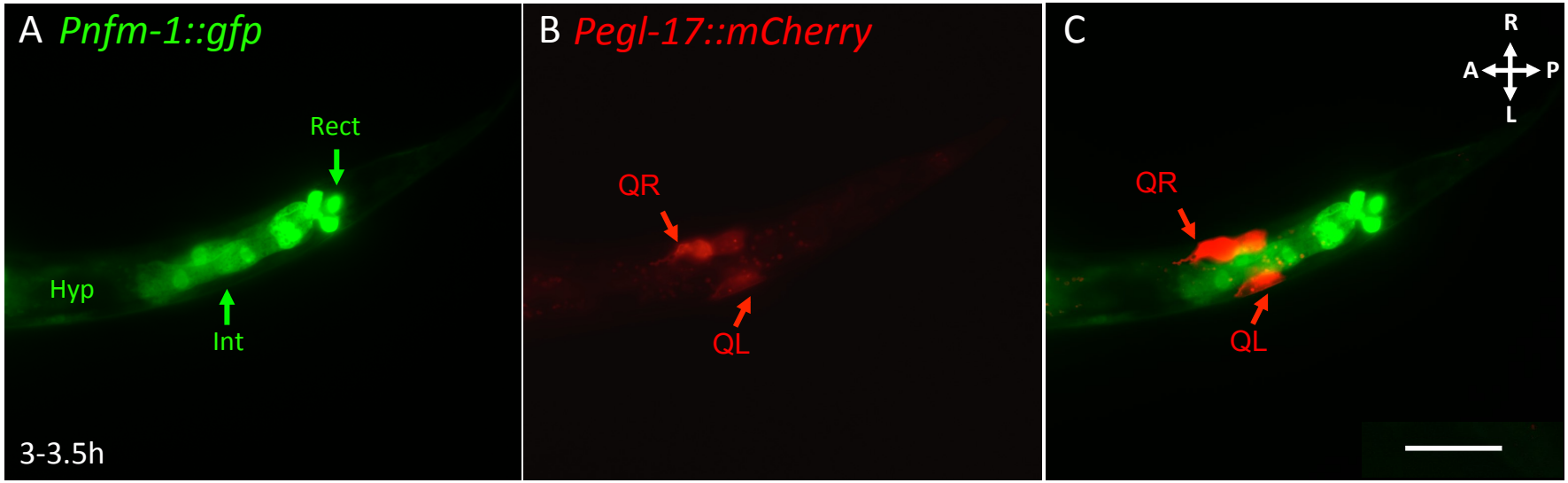
A Pnfm-1::gfp
Rect
Hyp
Int
3-3.5h
B Pegl-17::mCherry
QR
QL
C
R
A
P
L
QR
QL

Fig. 5

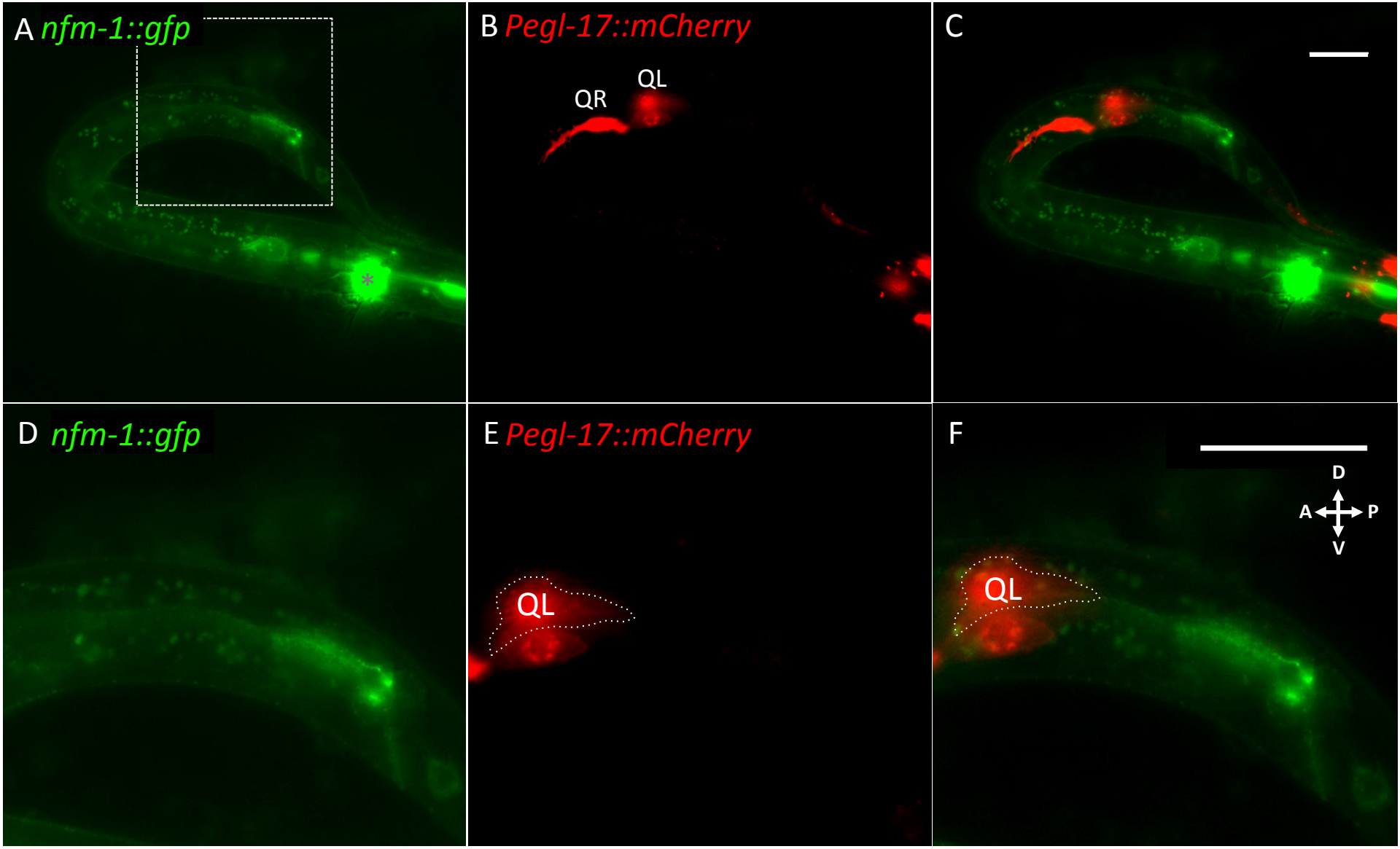
A nfm-1::gfp
B Pegl-17::mCherry
QR
QL
C
D nfm-1::gfp
E Pegl-17::mCherry
QL
F
D
A
P
V
QL

Fig. 6

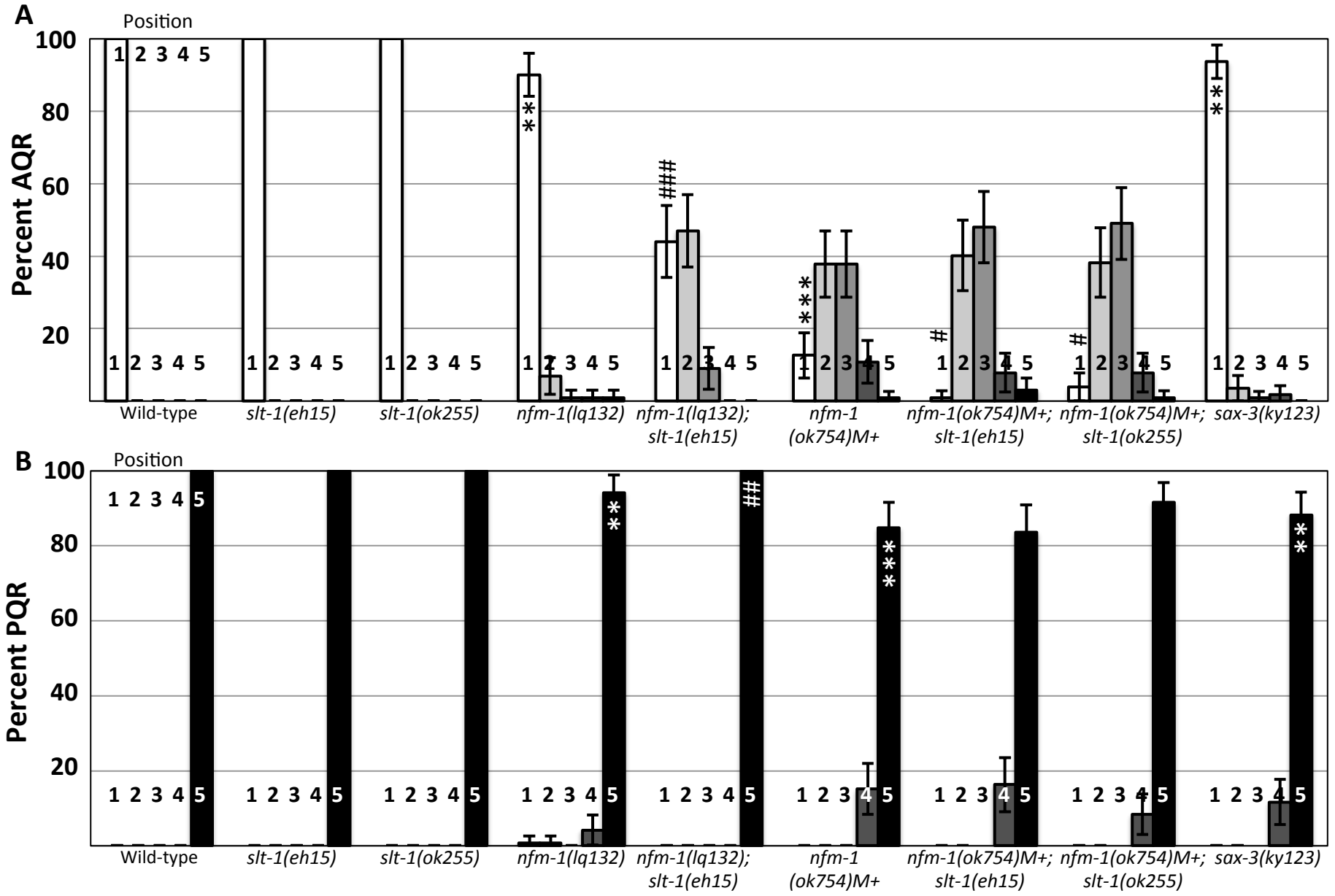

Fig. 7

N≥100

*p<0.05, **p<0.005,***p<0.0005 compared to wild-type

#p<0.05, ##p<0.005, ###p<0.0005 compared to corresponding *nfm-1* mutant